Critical Current Oscillations in Strong Ferromagnetic π Junctions

J. W. A. Robinson,[1] S. Piano,[1,2] G. Burnell,[1] C. Bell,[3] and M. G. Blamire[1]

[1]*Department of Material Science, University of Cambridge, Pembroke Street, Cambridge CB2 3QZ, United Kingdom*
[2]*Physics Department, CNR-Supermat Laboratory, University of Salerno, Via S. Allende, 84081 Baronissi (SA), Italy*
[3]*Kamerlingh Onnes Laboratory, Leiden University, P.O. Box 9504, 2300 RA Leiden, The Netherlands*

(Received 2 June 2006; published 25 October 2006)

We report magnetic and electrical measurements of Nb Josephson junctions with strongly ferromagnetic barriers of Co, Ni, and $Ni_{80}Fe_{20}$ (Py). All these materials show multiple oscillations of critical current with a barrier thickness implying repeated 0-π phase transitions in the superconducting order parameter. We show, in particular, that the Co barrier devices can be accurately modeled using existing clean limit theories and that, despite the high exchange energy (309 meV), the large I_cR_N value in the π state means Co barriers are ideally suited to the practical development of superconducting π-shift devices.

DOI: 10.1103/PhysRevLett.97.177003 PACS numbers: 74.50.+r, 74.25.Ha, 74.25.Sv, 74.78.Db

Although the interplay of superconductivity and ferromagnetism has been the subject of study for many decades [1], theoretical and experimental investigations into the properties of superconductor-ferromagnetic metal (S/F) heterostructures have seen an upsurge in interest in recent years following the experimental observation of 0-π transitions in the superconducting order parameter in S/F thin films by Ryazanov *et al.* [2] and by Kontos *et al.* [3]. In terms of the Josephson relationship $I_c = I_0 \sin\Delta\phi$, where $\Delta\phi$ is the phase difference between the two S layers, a transition from the 0 to π states implies a change in sign of I_0 from positive to negative. A change in sign of I_0 is a consequence of a phase change in the electron pair wave function induced in the F layer by the proximity effect. It is possible to describe the I_c dependence with ferromagnetic thickness (d_F) by the generic expression

$$I_cR_N(d_F) \propto I_cR_N(d_0)\left|\frac{\sin\frac{d_F-d_1}{\xi_2}}{\sin\frac{d_1-d_0}{\xi_2}}\right|\exp\left\{\frac{d_0-d_F}{\xi_1}\right\}, \tag{1}$$

where d_1 is the thickness of the F layer corresponding to the first minimum and $I_cR_N(d_0)$ is the first experimental value of I_cR_N (R_N is the normal state resistance). Transitions can be observed as oscillations in the critical temperature (T_c) of S/F multilayers [4–7] as well as oscillations in the I_c of S/F/S junctions with both thickness of the F layer, d_F [8–10] and, for weak ferromagnets whose exchange energy (E_{ex}) is comparable to k_BT_c of the superconductor, with temperature [11].

The majority of studies of S/F/S structures have concentrated on the use of weak ferromagnets, such as Cu_xNi_{1-x} and Pd_xNi_{1-x}, where the temperature dependence can be observed and where d_F over which oscillations in T_c or I_c are observed can be comparatively large. Even where strong ferromagnets have been used, a significant magnetic "dead" layer corresponding to a loss in total moment [12] is usually observed which complicates the modeling—see Table I.

In the dirty limit where the mean free path $L < d_F$ and $L < \hbar v_f/E_{\mathrm{ex}}$ the two decay lengths, ξ_1 and ξ_2, take similar values and so multiple oscillations of I_c are not observed. In contrast, in the clean limit where $d_F < L$ and $L > \hbar v_f/E_{\mathrm{ex}}$ the decay of the envelope determining the modulation amplitude (ξ_1) can be much larger than the oscillation period (ξ_2). Most previous studies, including those using strong ferromagnets, have been performed in the dirty limit; for practical applications, in which large I_cR_N values are required in the π state, it is vital to develop high quality clean limit S/F/S devices. A recent report using the ferromagnetic intermetallic Ni_3Al shows I_c oscillations in the clean limit [13], but with a very large magnetic dead layer which is not accounted for in any phenomenological model and which is likely to make practical control of the phase state of the junction difficult.

Co is a proven device material which can be deposited in clean thin film form with accurately controlled thickness; however, it has not been previously applied in S/F/S junctions because the exchange energy was considered to be far too large. In this Letter, we report for the first time measurements of junctions containing Co barriers, together with comparative studies of Py and Ni barriers. We show that, unlike Py and Ni and the weak ferromagnets, the Co data fit excellently to clean limit theory. As importantly, the

TABLE I. A summary of reported parameters for different material systems. DL stands for "Dead Layer Thickness" and * "This Letter".

ξ_1 (nm)	ξ_2 (nm)	F	v_F (ms^{-1})	E_{ex} (meV)	DL (nm)	Reference
1.2	1.6	$Ni_{20}Fe_{80}$	2.2×10^5	95	0.7	[9]
1.4	0.46	$Ni_{20}Fe_{80}$	2.2×10^5	201	0.5	*
1.8	2.0	$Pd_{90}Ni_{10}$	2.0×10^5	35	⋯	[3]
1.7	1.0	Ni	2.8×10^5	200	⋯	[10]
2.3	0.86	Ni	2.8×10^5	107	⋯	[8]
4.1	1.2	Ni	2.8×10^5	80	1.5	*
4.6	0.45	Ni_3Al	1.5×10^5	86	5–8	[13]
3.0	0.3	Co	2.8×10^5	309	0.8	*

magnetic dead layer in the Co is less then 1 nm allowing precise control of the phase state of Nb/Co/Nb π junctions.

Nb/Co/Nb, Nb/Py/Nb, and Nb/Ni/Nb films were deposited on 10×5 mm silicon (100) substrates with a 250 nm thermal oxide. Simultaneous to growing 10×5 mm thin films for patterning, identical 5×5 mm films were deposited for magnetic characterization in a vibrating sample magnetometer (VSM). Films were deposited by dc magnetron sputtering at 1.5 Pa and the deposition system was baked out for seven hours and subsequently cooled with liquid nitrogen for 1 h prior to the deposition, which gave a base pressure better than 5×10^{-6} Pa and an oxygen partial pressure of less than 3×10^{-9} Pa. The deposition rates are $1.2\ \mathrm{nm\,min}^{-1}$ for Co, $1.6\ \mathrm{nm\,min}^{-1}$ for Py, $0.4\ \mathrm{nm\,min}^{-1}$ for Ni, $2.4\ \mathrm{nm\,min}^{-1}$ for Cu, and $12.6\ \mathrm{nm\,min}^{-1}$ for Nb. In a single deposition run, multiple silicon substrates were placed on a rotating holder which passed in turn under three magnetrons. The thickness of each layer was controlled by setting the angular speed at which the substrates moved under the respective targets and by setting the target power. When depositing the F barriers, an acceleration curve was programmed which allowed the angular speed of the substrates to change as they passed under the relevant targets so that d_F was dependent on the substrate position, θ, on the rotating holder. With knowledge of the deposition parameters, the rotation was programmed such that $d(d_F)/d\theta$ was a constant. This method of varying d_F guaranteed that all interfaces were prepared under the same conditions. To confirm control over d_F we performed x-ray reflectivity of Nb/Co/Nb thin films where $d_{\mathrm{Nb}} \simeq 5$ nm and d_{Co} was varied from 0.5 nm to 5.0 nm. Low angle x-ray scans were made and the observed d_{Co} ($d_{\mathrm{Co(observed)}}$) extracted by fitting the period of the Kiessig fringes using a simulation package. It was found that $d_{\mathrm{Co(expected)}}$ was well correlated with $d_{\mathrm{Co(observed)}}$ with a mean deviation of 0.2 nm.

To help locate the F barrier in subsequent focused ion beam (FIB) processing, a thin (20 nm) Cu layer was embedded in the 250 nm thick Nb electrodes located 50 nm from the F layer (where $50\ \mathrm{nm} > \xi_{\mathrm{Nb}}$). At 20 nm, $d_{\mathrm{Cu}} \ll \xi_{\mathrm{Cu}}$ and is therefore totally proximitized by the Nb and plays no part in the electrical properties of the junctions. d_{Co} and d_{Py} were varied from $\simeq 0.5$ nm to $\simeq 5$ nm and d_{Ni} was varied from $\simeq 1.0$ nm to $\simeq 10$ nm. The films were patterned using optical lithography, followed by Ar ion milling ($3\ \mathrm{mA\,cm}^{-2}$, 500 V beam) to produce micron scale tracks and contact pads, to allow four-point measurements to be performed. These tracks were then patterned with a Ga^{+} FIB (Philips/FEI FIB 200) to achieve vertical transport [see inset Fig. 2(a)] with a device area in the 0.2–1 $\mu\mathrm{m}^2$ range [14].

The magnetic moment per unit surface area of the films was measured at 300 K using a VSM (see Fig. 1) and reveals magnetic dead layers, DLs, of $\simeq 0.75$ nm for Co, $\simeq 0.5$ nm for Py and $\simeq 1.5$ nm for Ni. DL is attributed to lattice mismatch, formation of amorphous interfaces, and a breakdown in the crystal structure leading to a reduced exchange interaction between neighboring atoms and a reduction in T_{Curie} and E_{ex} [15–17]. In the case of Co and Ni, both the thickness of DL and the total moments for a given thickness greater than the DL are close to those reported in systematic studies Nb/F bilayers [6,18].

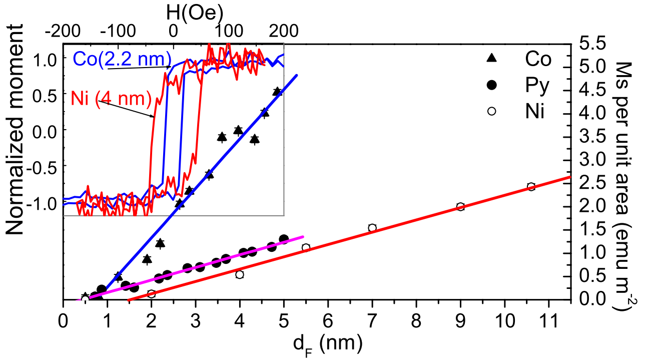

FIG. 1 (color online). Magnetic moment per unit area vs Co, Py, and Ni thickness at 300 K. Inset: hysteresis loops for Co and Ni.

Transport measurements were made in a liquid He dip probe. The differential resistance as a function of bias current, $dV/dI(I)$, of the junctions was measured with a lock-in technique. I_c was defined as the point where $dV/dI(I)$ increases above the value for zero bias current. R_N was measured using a quasi-dc bias current of 3–5 mA; this enabled the nonlinear portion of the I-V curves to be neglected, but was not large enough to drive the Nb electrodes into a normal state. A $dV/dI(I)$ and $V(I)$ plot for a typical Nb-Py-Nb junction is shown inset of Fig. 2(b). The I_c of the devices ranged from 500 μA to below the minimum sensitivity of our apparatus (50 nA), while the R_N was in the range 1.0–100 mΩ.

I_cR_N as a function of Co, Py, and Ni thickness at 4.2 K is shown in Figs. 2(a)–2(c). Each point in these figures corresponds to the mean of several junctions with different areas; the vertical error bars are derived from the measured variation in I_cR_N and a small noise contribution due to the current source. From x-ray reflectivity results, as discussed above, we take the error in d_F for all F barriers to be $\simeq$ 0.2 nm. All of the devices shown in this data set presented Shapiro steps upon the application of microwaves and an I_c modulation with applied field H_A. As expected, I_cR_N for the Co, Py, and Ni decreases exponentially and in an oscillatory fashion with d_F.

The Co data were modeled using Eq. (1); from the model fit shown in Fig. 2(a) we find that the period of the Co oscillations is $\simeq 1.9$ nm, hence $\xi_2 \simeq 0.3$ nm and $\xi_1 \simeq$ 3.0 nm. This gives a ξ_2/ξ_1 ratio of $\sim$0.11. A theoretical treatment involves solving linear Eilenberger equations [19] and gives Eq. (2)

$$\tanh\frac{L}{\xi_{\mathrm{eff}}} = \frac{\xi_{\mathrm{eff}}^{-1}}{\xi_0^{-1} + L^{-1} + i\xi_H^{-1}}, \tag{2}$$

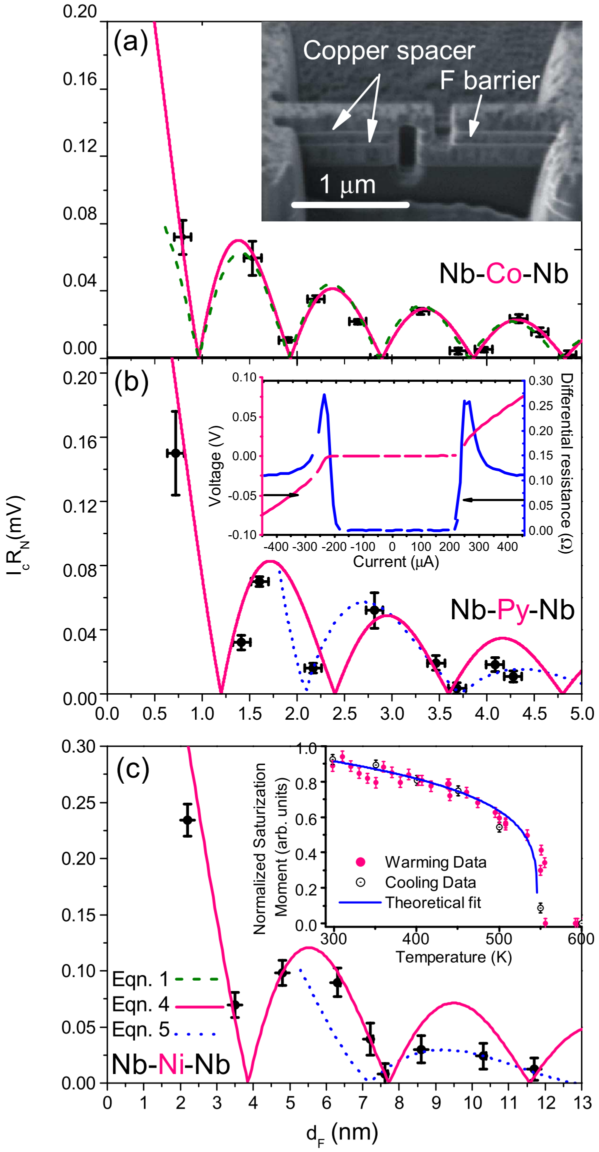

FIG. 2 (color online). I_cR_N as a function of Co, Py, and Ni thickness at 4.2 K. Inset (a) an FIB micrograph of a typical Nb-Co-Nb Josephson junction. Inset (b) $V(I)$ and $dV/dI(I)$ plotted for a Nb/Py/Nb Josephson junction. Inset (c) $M(T)$ as a function of warming and cooling temperature for a Nb/Ni/Nb trilayer where $d_{\mathrm{Ni}} \simeq 9$ nm.

where ξ_{eff} is the effective decay length given by $\xi_{\mathrm{eff}}^{-1} = \xi_1^{-1} + i\xi_2^{-1}$, ξ_0 is the Ginzburg-Landau coherence length, and ξ_H is a complex coherence length. In the clean limit $1 + L\xi_0^{-1} \gg \frac{1}{2}\max\{\ln(1 + L\xi_0^{-1}), \ln(L\xi_H^{-1})\}$. The solution of Eq. (2) gives

$$\xi_1^{-1} = \xi_0^{-1} + L^{-1}, \quad \xi_0 = \frac{v_F\hbar}{2\pi T_c k_B}, \quad \xi_2 = \xi_H = \frac{v_F\hbar}{2E_{\mathrm{ex}}}, \tag{3}$$

and the numerical solution is shown in Fig. 3.

Following the method of Gusakova and Kupriyanov [19] we find from Fig. 3 that the experimental ratio $\xi_2/\xi_1 \simeq 0.1$ corresponds to two inverse magnetic lengths of $L/\xi_H \simeq 16.5$ and $L/\xi_H \simeq 18.7$. By assuming $L/\xi_0 \simeq 0.1$ and for the estimated parameters $\xi_1 \simeq 3$ nm and $\xi_2 \simeq 0.3$ nm we obtained, from the inset in Fig. 3, that for $L/\xi_H \simeq 16.5$ and $L/\xi_H \simeq 18.7$, $\bar{L} \simeq 5$ nm. Inputting these values into Eq. (3) gives $v_F(\mathrm{Co}) \simeq 2.8 \times 10^5$ ms^{-1} which is similar to other reported values of $v_F(\mathrm{Co})$ [20] and $E_{\mathrm{ex}} \simeq 309$ meV. As a comparison we have also modeled the Co oscillations with a simpler theoretical model given by Eq. (4) [21]

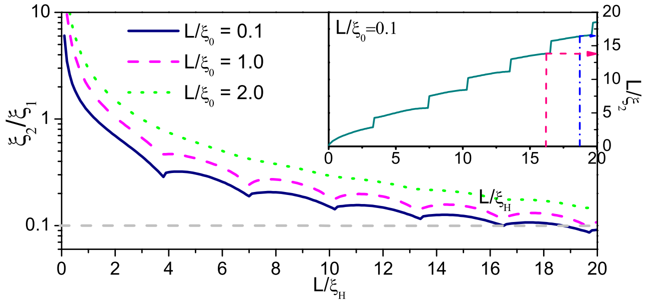

FIG. 3 (color online). The dependence of ξ_2/ξ_1 with inverse magnetic length, L/ξ_H, calculated for different ratios of L/ξ_0. Inset: inverse decay length, $L/\xi_2 = f(L/\xi_0)$, for when $L/\xi_H \simeq 0.1$.

$$I_cR_N \propto \frac{|\sin(2E_{\mathrm{ex}}d_F/\hbar v_f)|}{2E_{\mathrm{ex}}d_F/\hbar v_f}. \tag{4}$$

As in the case of Eq. (1) the fitting between the theoretical model and the experimental data is good [see Fig. 2(a) dashed line] and, in particular, the best fitting has been obtained by using $v_F = 2.8 \times 10^5$ ms^{-1} and $E_{\mathrm{ex}} = 309$ meV.

In the case of Py, Eq. (4) closely matches the experimental data up to a thickness of $\simeq 3.6$ nm and in the case of Ni, the oscillations follow the clean limit theory to $\simeq 7$ nm. Above these values a better fit is obtained using a formula for a diffusive and high E_{ex} ferromagnet [22]:

$$I_CR_N \propto \left| \mathrm{Re} \sum_{\omega_m > 0} \frac{\Delta^2}{\Delta^2 + \omega_m^2} \int_{-1}^{1} \frac{\mu}{\sinh(k_\omega d_F/\mu L)} d\mu \right|, \tag{5}$$

where Δ is the superconducting energy gap, ω_m is the Matsubara frequency and is given by $\omega_m = \pi T k_B(2m + 1)$, where T is the transmission coefficient, and m is an integer number. $k_\omega = (1 + 2|\omega_m|\tau/\hbar) - 2iE_{\mathrm{ex}}\tau/\hbar$ and $\mu = \cos\theta$, where θ is the angle the momentum vector makes relative to the distance normal to the S/F interface. L is given by $v_f\tau$ and τ is the momentum relaxation time. For Eq. (4) the only fitting factor, besides the numerical prefactor, was the strength of the exchange interaction ($E_{\mathrm{ex}}/\hbar v_f$). In the case of Eq. (5) a suitable v_f, Δ, and E_{ex} had to be chosen. To fit Eq. (5) to Py and Ni data we used: $v_f(\mathrm{Py}) = 2.2 \times 10^5$ m/s and $L_{\mathrm{Py}} \simeq 2.3$ nm, and $v_f(\mathrm{Ni}) = 2.8 \times 10^5$ m/s and $L_{\mathrm{Ni}} \simeq 7$ nm and $\Delta = 1.3$ meV. These values are consistent with the ones used in Eq. (4) and elsewhere [8,9]. From the oscillation period,

$L_{\mathrm{osc}} \sim \hbar v_f/2E_{\mathrm{ex}}$, the E_{ex} of the Py and Ni barriers is estimated. We estimate $E_{\mathrm{ex}}(\mathrm{Py}) \simeq 201$ meV and $E_{\mathrm{ex}}(Ni) \simeq 80$ meV. $E_{\mathrm{ex}}(\mathrm{Py})$ is double that measured in Nb/Py/Nb junctions deposited with epitaxial barriers where $E_{\mathrm{ex}} \simeq 95$ meV [9]. $E_{\mathrm{ex}}(\mathrm{Ni})$ is close to other reported values by photoemission experiments [23]. The smaller than expected $E_{\mathrm{ex}}(\mathrm{Ni})$ is a consequence of impurities and possibly interdiffusion of Ni into Nb. For Ni, we have measured the magnetization saturation as a function of warming and cooling temperature [$M(T)$] [see inset of Fig. 2(c)] so that an estimate of $T_{\mathrm{Curie}}(\mathrm{Ni})$ could be made. The warming and cooling data follow each other implying that no interdiffusion has influenced the $M(T)$ curves. The warming data are modeled by the formula: $M(T)/M(0) = (1 - T/T_{\mathrm{Curie}})^{\beta}$, where $M(0)$ is the magnetization at absolute 0 K, T is the measuring temperature, and β and T_{Curie} are fitting parameters. We estimate $T_{\mathrm{Curie}} \simeq 571$ K, which is in agreement with T_{Curie} measurements of Ni in S/F bilayers [24]. This provides evidence that our Ni is consistent and not grossly degraded.

The fully clean limit behavior observed with the Co barriers arises most obviously from the use of a pure element, but also from the vertical coherence likely [25] even in noncrystalline heterostructures. The high E_{ex} results in a short oscillation period implying a need for Å-level control of layer thickness for practical devices; however, Co and Co alloys form the basis of current spintronic device production, and precision layer control and excellent compatibility with tunnel barriers [26] have been demonstrated in many industrial processes [27]. Co is an attractive material for qubits and other novel devices.

In summary, we have measured critical current oscillations in Co junctions as a function of Co barrier thickness which indicates that the devices are strongly in the clean limit. This results in higher I_cR_N values in the π state compared to I_cR_N values in the dirty limit. We also present complementary critical current oscillations through Py and Ni barriers. The oscillations in I_cR_N with d_F are indicative of 0-π crossovers and also show an excellent fit to theoretical models. We have estimated, from the periodicity of the oscillations, the exchange energies of the Co, Py, and Ni barriers to be 309 meV, 201 meV, and 80 meV, respectively. Results within this Letter are summarized in Table I alongside results reported elsewhere. Our results are not only interesting in their own right, but are a vital experimental step towards understanding the physics of quantum electronic devices based on superconductors and are of considerable value to the development of quantum information processing. Our devices are precursors to practical implementations into qubits and other applications in controllable and scalable superconducting quantum electronic devices.

The authors thank M. Yu. Kupriyanov, A. M. Cucolo, and F. Bobba for helpful discussions and N. Stelmashenko for technical assistance. We acknowledge the support of the EPSRC UK and the European Science Foundation π-shift network.

[1] A. I. Buzdin, Rev. Mod. Phys. **77**, 935 (2005).
[2] V. V. Ryazanov *et al.*, Phys. Rev. Lett. **86**, 2427 (2001).
[3] T. Kontos *et al.*, Phys. Rev. Lett. **89**, 137007 (2002).
[4] J. S. Jiang *et al.*, Phys. Rev. Lett. **74**, 314 (1995).
[5] Th. Mühge *et al.*, Phys. Rev. Lett. **77**, 1857 (1996).
[6] Y. Obi *et al.*, Physica (Amsterdam) **317–318C**, 149 (1999).
[7] L. Lazar *et al.*, Phys. Rev. B **61**, 3711 (2000).
[8] Y. Blum *et al.*, Phys. Rev. Lett. **89**, 187004 (2002).
[9] C. Bell *et al.*, Phys. Rev. B **71**, 180501(R) (2005).
[10] V. Shelukhin *et al.*, Phys. Rev. B **73**, 174506 (2006).
[11] H. Sellier *et al.*, Phys. Rev. B **68**, 054531 (2003).
[12] S. Pick, I. Turek, and H. Dreyssé, Solid State Commun. **124**, 21 (2002).
[13] F. Born *et al.*, Phys. Rev. B **74**, 140501(R) (2006).
[14] C. Bell *et al.*, Nanotechnology **14**, 630 (2003).
[15] J. Aarts *et al.*, Phys. Rev. B **56**, 2779 (1997).
[16] R. Zhang and R. F. Willis, Phys. Rev. Lett. **86**, 2665 (2001).
[17] Q. Leng *et al.*, J. Appl. Phys. **87**, 6621 (2000).
[18] J. E. Mattson, R. M. Osgood, C. D. Potter, C. H. Sowers, and S. D. Bader, J. Vac. Sci. Technol. A **15**, 1774 (1997).
[19] D. Yu. Gusakova, M. Yu. Kupriyanov, and A. A. Golubov, Pis'ma Zh. Eksp. Teor. Fiz. **83**, 487 (2006) [JETP Lett. **83**, 418 (2006)].
[20] D. Y. Petrovykh *et al.*, Appl. Phys. Lett. **73**, 3459 (1998).
[21] A. I. Buzdin, L. N. Bulaevskii, and S. V. Panyukov, JETP Lett. **35**, 178 (1982).
[22] F. S. Bergeret *et al.*, Phys. Rev. B **64**, 134506 (2001).
[23] P. Heinmann, F. J. Himpsel, and D. E. Eastman, Solid State Commun. **39**, 219 (1981).
[24] J. Kim, J. H. Kwon, K. Char, H. Doh, and H. Y. Choi, Phys. Rev. B **72**, 014518 (2005).
[25] C. W. Leung *et al.*, J. Magn. Magn. Mater. **269**, 15 (2004).
[26] I. I. Oleinik *et al.*, Phys. Rev. B **62**, 3952 (2000).
[27] C. Kaiser and S. S. P. Parkin, Appl. Phys. Lett. **84**, 3582 (2004).